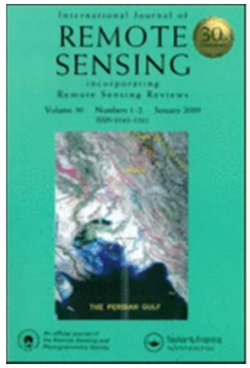

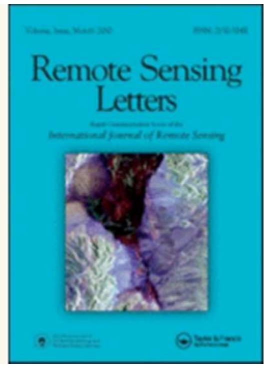

Effect of optically active substances and atmospheric correction schemes on remote sensing reflectance at a coastal site off Kochi

Journal:	*International Journal of Remote Sensing*
Manuscript ID:	TRES-SIP-2013-0049.R2
Manuscript Type:	IJRS Special Issue Paper
Date Submitted by the Author:	14-Nov-2013
Complete List of Authors:	Minu, P; Central Institute of Fisheries Technology (CIFT), Fishing Technology Division Lotliker, Aneesh; Indian National Centre for Ocean Information and Services (INCOIS), Advisory Services and Satellite Oceanography Group Shaju, S; Central Institute of Fisheries Technology (CIFT), Fishing Technology Division SanthoshKumar, B.; Central Institute of Fisheries Technology (CIFT), Fishing Technology Division Muhamed, Ashraf; Central Institute of Fisheries Technology (CIFT), Fishing Technology Division MeenaKumari, B; Indian Council of Agricultural Research (ICAR),
Keywords:	CHLOROPHYLL, ATMOSPHERIC CORRECTION, MODIS
Keywords (user defined):	Total Suspended Matter, Chromophoric Dissolved Organic Matter, Remote Sensing Reflectance

Effect of optically active substances and atmospheric correction schemes on remote sensing reflectance at a coastal site off Kochi

Minu P[1], Aneesh A. Lotliker[2*], S.S. Shaju[1], B. Santhosh Kumar[1], P. Muhamed Ashraf[1], B. Meenakumari[3]

[1]Central Institute of Fisheries Technology, ICAR, Matsyapuri P.O., Kochi 682 029, India
[2]Indian National Centre for Ocean Information Services (INCOIS), Ocean Valley, Hyderabad-500 090
[3]Indian Council of Agricultural Research (ICAR), Krishi Anusandhan Bhavan–II, Pusa, New Delhi 110 012
*Corresponding Author Email: aneesh@incois.gov.in

Abstract

The present study focused on understanding the variability of Optically Active substances (OAS) and its effect on the spectral remote sensing reflectance (R_{rs}). Further, the effect of atmospheric correction schemes on retrieval of chlorophyll_a (Chla) from satellite data was also analyzed. The OAS considered here are Chla, Coloured Dissolved Organic Matter (CDOM) and Total Suspended Matter (TSM). The satellite data from Moderate Resolution Imaging Spectroradiometer-Aqua (MODISA) was used for this study. The two atmospheric correction schemes considered were: Multi-scattering with 2-band model selection NIR correction (hereon referred as "A1") and MUMM correction and MUMM NIR calculation (hereon referred as "A2"). The default MODISA bio-optical algorithm (OC3M) was used for the retrieval of Chla. Analysis of OAS showed that Chla was the major light absorbing component with highly variable distribution (0.006 to 25.85 mg-m^{-3}). a_{CDOM}440 varied from 0.002 to 0.31 m^{-1} whereas the TSM varied from 0.005 to 33.44 mg-l^{-1}. The highest concentration of Chla was observed from August to November (i.e. end of southwest monsoon and beginning of northeast monsoon) which was attributed to the coastal upwelling. The average value of a_{CDOM}440 was found to be on the lower side of the global mean. A significant negative relationship between a_{CDOM}440 and salinity during southwest monsoon indicated that much of the CDOM during this season was from river discharge. The spectral R_{rs} was found to be strongly linked to the variability in Chla concentration indicating Chla was the major light absorbing component. The satellite derived spectral R_{rs} was in good agreement with *insitu* when Chla concentration was less than 5 mg-m^{-3}. The validation of Chla, derived from *insitu* R_{rs}, showed moderate performance (R^2=0.64, Log_{RMSE}=0.434, APD=43.6% and RPD=42.33%). However the accuracy of the algorithm was still within the acceptable limits. The statistical analysis for atmospheric correction schemes showed better 'r'(1.6), Log_{RMSE}(0.49), APD (25.46%) and RPD (17.57%) in the case of A1 as compared to A2. Whereas in the case of A2, R^2 (0.56), slope (0.26) and intercept (0.27) was better as compared to A1. The two atmospheric correction schemes did not show any significant statistical difference. However the default atmospheric correction scheme (A1) was found to be performing comparatively better probably due to the fact that the concentration of TSM and CDOM was much less to overcome the impact of Chla.

Key words: Chlorophyll, TSM, CDOM, Remote sensing reflectance, atmospheric correction, MODIS-Aqua

1. Introduction

The spectrum of radiation emerging out from the sea surface is significantly influenced by the presence of subsurface optically active substances (OAS). The major OAS encountered in the world ocean is phytoplankton pigment, chlorophyll (Chla), Coloured Dissolved Organic Matter (CDOM) and Total Suspended Matter (TSM). Chlorophyll absorbs in blue and red part of electromagnetic spectra whereas CDOM has strong absorption in shorter wavelengths. TSM contributes more towards scattering at longer wavelength.

In the perspective of ocean colour remote sensing, the ratio of water leaving radiance to downwelling radiance, termed as remote sensing reflectance (R_{rs}), is being used to estimate the concentration of various OAS present within the water column. O'Reilly et al. (1998 and 2000) established an empirical algorithm for satellite estimation of Chla using R_{rs}. However such bio-optical algorithms were primarily developed for case 1 waters where phytoplankton is solely responsible for the variation in R_{rs} (Gordon and Morel, 1983; Morel and Prieur, 1977; Siegel and Michaels, 1996; Stramski and Tegowski, 2001; Terrill et al., 2001; O'Reilly et al., 1998, 2000). These types of algorithms based on single models of Chla are inadequate for optically complex coastal and inland case 2 waters where substances other than phytoplankton, including TSM and CDOM has significant effect on R_{rs} (Bukata et al.,1995; IOCCG 2000). In case 2 waters, where R_{rs} get influenced by signal from CDOM and TSM, Chla often gets bias when estimated using such empirical algorithms (Ruddick et al., 2000; Siegel et al., 2000; Wang and Shi, 2005). On the other hand such empirical algorithms are computationally less intensive and easier for operational implementation. Moreover with advancements in ocean colour satellite sensors with more spectral bands, improved bio-optical algorithms and novel atmospheric correction models, has provided more accurate ocean colour products even in case 2 waters (Zibordi et al., 2006).

The accurate retrieval of Chla in case 2 waters also requires selection of suitable atmospheric correction scheme. In turbid waters the sensor derived R_{rs} at the blue wavelengths are often biased low and sometimes even go negative. This problem often results from assumptions that water leaving radiance is negligible at near-infrared (NIR) bands (Siegel et al., 2000). For the ocean-atmosphere system, the top-of-atmosphere (TOA) reflectance, $\rho_t(\lambda)$, measured by the satellite sensor, can be written as a linear sum from various contributions (ignore the white cap and sun glint):

$$\rho_t(\lambda) = \rho_r(\lambda) + \rho_a(\lambda) + t(\lambda)\rho_w(\lambda) \quad (1)$$

where $\rho_r(\lambda)$, $\rho_a(\lambda)$ and $\rho_w(\lambda)$ are the reflectance contributions from molecules (Rayleigh scattering), aerosols (including Rayleigh-aerosol interactions) and ocean waters, respectively. $t(\lambda)$ is the diffuse transmittance of the atmosphere. The goal of ocean colour remote sensing is accurate retrieval of water-leaving reflectance ρw (λ) by eliminating the contribution from atmospheric radiance (ρr (λ) and ρa (λ)) and ocean surface effects. The contribution of atmospheric radiance to total signal received by the visible satellite sensor is approximately 85%. In the default iterative atmospheric correction scheme, used by many sensors, ocean is assumed to be dark at near infra-red (NIR) bands (748 and 869 nm). This black pixel assumption (BPA) is used for initial iteration and relaxed progressively. However the initial BPA in the NIR region is invalid for turbid waters, leading to significant errors in retrieval of Chla (Siegel et al., 2000; Ruddick et al 2000).

The quality of the data products derived from the ocean color satellite largely depend upon accurate atmospheric correction scheme and suitable bio-optical algorithm. Hence the present research work has been carried out with objectives: 1) understanding effect of OAS on R_{rs}, 2) validation of operational bio-optical algorithm (OC3M) for retrieval of Chla and 3) to understand the effect of atmospheric correction schemes on retrieval of R_{rs} and Chla.

2. Study area

The present study has been carried out in coastal waters off Kochi, southwest coast of India which is connected by backwaters (Fig. 1). The study area is largely influenced by the fresh water discharge and seasonally reversing monsoon. The summer (southwest) monsoon extends from June to September whereas the winter (northeast) monsoon extends from December to March. During the transition phase of northeast to southwest monsoon, the study area experiences strong vertical mixing due to wind induced upwelling along with a northward undercurrent and a southward surface flow (Kumar and Kumar, 1996). During this period primary production ranging from 12.0 to 648.0 mg Cm-2d-1 was reported (Sarupria and Bhargava, 1993; Habeebrehman et al., 2008). Upwelling process supported by the southerly current observed along the coastal waters during southwest monsoon results in maximum fluctuation in primary production ranging between 40.0 to 1225.0 mg Cm-2 d-1 (Sarupria and Bhargava, 1993; Habeebrehman et al., 2008; Joshi and Rao, 2012). After southwest monsoon, the hydrographic parameters change causing very strong fresh water discharge from backwaters and this results in lowest primary production in the area, ranging from 21.0 to 263.0 mgCm^{-2} d^{-1} (Sarupria and Bhargava, 1993; Srinivas and Dinesh Kumar, 2006; Habeebrehman et al., 2008). The study area draw special attention because of the occurrence of witness seasonal Mudbanks at certain locations, during southwest monsoon period (Balachandran, 2004), and also phytoplankton blooms (Srinivas and Dineshkumar, 2006).

3. Data and Methodology

3.1. Sampling

The sampling was conducted at eight stations for all months from 2009 to 2011 except for few months in the southwest monsoon. The sampling was carried out using Commercial Purse seiner. The selection of stations was based on the bathymetry and were scattered equally on either side of the backwater outlet. The surface water samples were collected using 2.5 L Hydro-Bios Niskin plastic water sampler. At each station SatlanticTM hyperspectral radiometer (HyperOCRII) was operated for the measurement of R_{rs}. Subsequently water samples were also collected for the estimation of Chla concentration, CDOM absorption and TSM concentration. Total 63 sampling points were available for the analysis.

3.2. Data Analysis

Chla was measured using Turner Designs™ 10 AU-field fluorometer following Welschmeyer method (Welschmeyer 1994). Between 0.1 and 1 L of water were filtered onto 25 mm Glass Fibre Filters (GF/F) using a vacuum pressure of <200 mm Hg and extracted overnight in 90% acetone. The samples were then centrifuged for 10-20 min at 2000 rpm and the raw fluorescence given as digital volts were converted into Chla concentrations using calibration curves from Chla standards (Sigma-Aldrich Company Ltd.).

TSM was determined gravimetrically according to Strickland and Parsons (1972) and JGOFS protocols (UNESCO 1994). In brief, the water samples were filtered through 0.45 µm pre-weighed polycarbonate filter paper, then washed with distilled water and immediately dried in an oven at 75°C. They were then re-weighed in the laboratory using an electronic balance.

Absorption due to CDOM (a_{CDOM}) was measured spectrophotometrically following Kowalczuk and Kaczmarek (1996). Water samples were filtered onboard through 0.2 µm Sartorious cellulose membrane filters. The sample transparency was measured using Shimadzu™ double beam UV-2450 spectrophotometer, over the spectral range 400 to 700 nm at 1 nm resolution, in 10 cm quartz cuvette against MilliQ water as a blank. a_{CDOM} was calculated from the optical density of the sample and path length following the methods given in Twardowski et al. (2004).

3.3. Insitu R_{rs}

The remote sensing reflectance (R_{rs}) in Hyperspectral bands were measured using Satlantic™ hyperspectal radiometer (HyperOCRII). The instrument contains 256 optical channels between 350 to 800 nm that measures downwelling surface irradiance (E_S) and profiles of downwelling irradiance (E_d) and upwelling radiance (L_u). The radiometers were deployed away from the vessel to avoid ship-induced perturbations and shading (Fargion and Mueller, 2000). The data were recorded using SatView™ software and processed using Prosoft™ software. When the tilt of the sensor was > 5^0 and profiling velocity was more than 0.7 $m\text{-}s^{-1}$ the data were discarded to ensure high quality of the measurements. The $R_{rs}(\lambda)$ was then calculated from

$$R_{rs}(\lambda) = \frac{L_w(\lambda,0^+)}{E_d(\lambda,0^+)} \quad (2)$$

Where $E_d(\lambda,0^+)$ is the above surface downwelling spectral irradiance ($Wm^{-2}nm^{-1}$) and $L_w(\lambda,0^+)$ is the water leaving radiance ($Wm^{-2}nm^{-1}sr^{-1}$). Standard ocean optics protocols (Fargion and Mueller, 2000) were used in the computation of water leaving radiance (L_w):

$$L_w(\lambda,0^+) = L_u(\lambda,0^-)\frac{[1-\rho(\lambda,\theta)]}{\eta_w^2(\lambda)} \quad (3)$$

Where $L_u(\lambda,0^-)$ is water leaving radiance below surface, $\rho(\lambda,\theta)$ is Fresnel reflectance index of seawater and $\eta_w(\lambda)$ is Fresnel refractive index of seawater.

Surface downwelling irradiance was calculated from:

$$E_d(\lambda,0^+) = \frac{E_d(\lambda,0^-)}{1-\alpha} \quad (4)$$

Where α is the Fresnel reflection albedo from sun (~0.043), and $E_d(\lambda,0^-)$ is extrapolated from $E_d(\lambda, z)$ profile.

3.4. Satellite data Processing

Moderate Resolution Imaging Spectroradiometer – Aqua (MODISA) level-0, data corresponding to the days of *insitu* data, were acquired from GSFC-NASA (http://oceancolor.gsfc.nasa.gov). The data were processed from Level-0 to Level-2, using Sea Viewing Wide Field of view Sensor (SeaWiFS) Data Analysis System (SeaDAS) software with two atmospheric correction schemes. The two atmospheric correction schemes chosen were: 1) Multi-scattering with 2-band model selection NIR correction (from hereon referred as: A1) (Siegel et al., 2000) and 2) Multi-scattering with MUMM correction and MUMM NIR calculation (from hereon referred as: A2) (Ruddick et al., 2000). The first atmospheric correction scheme is used as default for MODIS– Aqua. The default bio-optical algorithm (OC3M) was used for the retrieval of Chla. The satellite match-up data for Chla and R_{rs} at wavelengths 412, 443, 469, 488, 531, 555, 645, 667 and 678 were extracted from 3 X 3 pixel box (Bailey and Werdell, 2006). Subsequently the quality of the match-up data was assessed as per ocean optic protocol (Fargion and Muller, 2000) and 13 match-up points were selected for validation.

4. Results

4.1. Distribution of OAS in the study area

The preliminary analysis of the study includes understanding the variability in distribution of OAS such as Chla, $a_{CDOM}440$ and TSM. The distribution of OAS for the entire sampling period was analyzed using frequency distribution plots (Fig. 2). The results showed large variability in the distribution of Chla and TSM. Chla ranged between 0.006 to 25.85 mg-m^{-3} whereas the concentration of TSM ranged from 0.005 to 33.44 mg-l^{-1}. The $a_{CDOM}440$ ranged between 0.002 to 0.31 m^{-1}. The distribution of Chla did not show any specific trend in terms of magnitude. The maximum in the distribution of $a_{CDOM}440$ was seen at the median frequency ranging from 0.1 to 0.15 m^{-1} with lower values occurring more frequently as compared to higher. The distribution of TSM showed higher frequency at lower concentrations (< 4.0 mg-l^{-1}).

The analysis carried out using frequency distribution plots has given an insight about overall distribution of OAS sampled during the study period. However it is also important to understand the variability of these OAS on the temporal scale. To achieve this, the variability in the distribution of OAS was analyzed at monthly scale. All the spatial data corresponding to one month was averaged and presented in Fig. 3 along with the standard deviation.

The monthly mean Chla concentration was found to be varied between 3.85 to 12.49 mg-m^{-3}. The highest concentration was observed during the end of southwest monsoon and prior to onset of northeast monsoon (i.e. from August to November). The concentration of Chla was significantly lower during February to May corresponding to later phase of northeast monsoon. Also high standard deviation was observed throughout the study period. The spatial mean of $a_{CDOM}440$ did not show any significant trend at monthly scale. The values encountered in the present study were also on the lower side of the global mean as reported by Siegel et al. (2002). The $a_{CDOM}440$ reached peak during northeast monsoon (i.e in the month of January) with a mean value of 0.13 ± 0.08 m^{-1}. The TSM concentration showed large variability at the temporal scale with a maximum of 28.58 ± 1.14 mg-l^{-}1 for the month of March 2009. The overall trend showed that TSM was high prior to onset of southwest monsoon. Also the standard deviation was very low except for two months (September and January 2011).

4.2. Effect of Chla on R_{rs}

This section intends towards analyzing effect of OAS on spectral R_{rs}. Further the variability in R_{rs} derived using two different atmospheric correction schemes (A1: Multi-scattering with 2-band model selection NIR correction and A2: Multi-scattering with MUMM correction and MUMM NIR calculation) has also been assessed. The spectral variability of *insitu* (solid line) and satellite derived R_{rs} using A1 (triangles) and A2 (circles) are presented in Fig 4. Although we had total 63 data points, only those stations where satellite matchup was available are presented here. The plots were arranged with the increasing concentration of Chla. Even though the magnitude of satellite derived spectral R_{rs} doesn't match, in most of the cases, the shape of the spectra seems to be in good agreement with the *insitu*. At lower concentration of Chla (S57), R_{rs} was maximum at the shorter wavelength and decreased exponentially towards longer wavelength. Further it was also observed that with increasing concentration of Chla, peak R_{rs} was shifted towards longer wavelength.

While looking at the satellite derived spectral R_{rs} using A1 and A2, it was observed that A1 was higher than A2 in all the cases. Also spectral R_{rs} derived using atmospheric correction scheme, A1, was found to be in better agreement with *insitu*. Further the spectral R_{rs} derived using atmospheric correction scheme, A2, found to be underestimating in all the cases. The R_{rs} spectra appropriately fitted in Chla concentrations <5 mg-m^{-3} whereas in concentrations >5 mg-m^{-3}, it seems to be slightly overestimated. In cases where Chla concentration is > 12 mg- m^{-3} the satellite derived R_{rs} spectra was underestimated. However no trend was observed in variability of TSM and a_{CDOM}440 with spectral R_{rs}.

4.3. Validation of Chla

In this section an attempt has been made to evaluate the effect of two atmospheric correction schemes on retrieval of Chla using default bio-optical algorithm. Prior to this the bio-optical algorithm was also validated. To do this *insitu* R_{rs}, measured using radiometer, was used so as to ignore the effect of atmospheric contribution. Chla estimated using radiometric R_{rs}, by applying OC3M algorithm, was validated against the Chla estimated from water sample analysis. The results are shown in Fig. 5a. The validation statistics are given in Table 1. The results showed that both are closely matched with good correlation (R^2=0.64). The Log_{RMSE} was 0.43. The absolute and relative percentage error was on the higher side (APD=43.6 % and RPD=42.33%).

Fig. 5b and 5c showed the correlation between *insitu* measured Chla and that derived from MODISA using A1 and A2 atmospheric correction schemes. In general 77% of the data points were within 95% confidence limit. The statistical indicators (Table 1) showed comparable correlation coefficients of 0.54 and 0.56 for A1 and A2 respectively. The intercept was low in case of A2 (0.27) as compared to that of A1 (0.4). Chla derived using A1 showed low 'r' value (1.6) as compared to that from A2 (2.18). Further the APD and RPD were also lower in case of Chla derived using A1. The overall statistical indicators showed better 'r', RMSE, APD and RPD in the case of A1 as compared to A2, whereas in the case of A2, R^2, slope and intercept was better as compared to A1.

5. Discussion

The present study is focused on two major objectives. The first one is to understand the variability of OAS in the area subjected to strong monsoonal forcing. The second one is to evaluate the effect of atmospheric scheme on retrieval of R_{rs} and Chla from satellite data. The first objective was addressed by analyzing frequency distribution of OAS throughout the period of the study and also by understanding its spatial and temporal variability on monthly scale. The results of the analysis showed large variability in distribution of Chla. The a_{CDOM}440 was less than the global mean as reported by Siegel et al. (2002). Further maximum frequency for TSM was observed at the lower concentration. This clearly indicates that Chla is the primary substance that can affect the distribution of light and hence R_{rs}. Further the high concentration of Chla was encountered during end of southwest monsoon and prior to onset of northeast monsoon. The earlier studies carried out by Le´vy et al. (2007) clearly showed that the Chla peaks during August-September along southwestern coast of India. This elevated concentration of Chla was attributed to the intense coastal upwelling occurring during the southwest monsoon. During southwest monsoon the West Indian Coastal Currents (WICC) changes the direction towards south resulting in the coastal upwelling (Shankar et al., 2002). Further the upwelling process also results in high primary production ranging between 40.0 to 1225.0 mg Cm^{-2} d^{-1} (Joshi and Rao, 2012).

In the present study distribution of a_{CDOM}440 and TSM were highly variable at the temporal scale. However the average value of a_{CDOM}440 was found to be on the lower side of the global mean. The distribution of CDOM and TSM has been further analyzed by correlating with salinity at seasonal scale. During southwest monsoon season strong negative correlation (R=-0.6) was observed between a_{CDOM}440 and salinity. However during other months a_{CDOM}440 did not correlate significantly with the salinity. The river discharge is the major contributor of CDOM in the coastal waters. Apart from these resuspension and *insitu* degradation can also enhance CDOM (Menon et al., 2011). Similarly the potential source of TSM is either from river or due to resuspension in shallow waters. The coastal waters off Kochi is subjected to upwelling and heavy fresh water discharge from the adjacent estuary during southwest monsoon period which enhances nutrient upload resulting in the increased biological production (Nair et al., 1992; Jyothibabu et al., 2006). This indicates that much of the CDOM during southwest monsoon is from river discharge. Also there was no significant relationship between a_{CDOM}440 and TSM. Further a lag in the elevation of Chla concentration and a_{CDOM}440, during non monsoon months, indicates that during these months, CDOM could be principally due to the *insitu* degradation of phytoplankton. Although TSM distribution showed higher frequency at the lower concentration, the maximum concentration was during southwest monsoon. Further TSM did not show any significant relation with salinity. Some of the previous studies by Thomas et al. (2004), Srinivas et al. (2003) and Jyothibabu et al. (2006) also reported that continuous dredging process occurring throughout the year in the study area increases the nutrient and sediment load in the estuary which is drained into the coastal waters.

The spectral R_{rs} is the basis for the empirical bio-optical algorithm (O'Reilly et al., 1998 and 2000). The spectral R_{rs}, in the present study were found to be strongly linked to the variability in Chla concentration. It was observed that with increase in Chla concentration, the peak R_{rs} was shifted to the longer wavelength. This is analogous to the previous studies which formed the basis for the development of empirical band-ratio algorithm for the retrieval of Chla from satellite data (O'Reilly et al., 1998 and 2000). While analyzing the R_{rs} derived using two atmospheric correction schemes (A1 and A2), A1 was closer to the measured R_{rs}. In the case of A1, Gordon and Wang (1994) showed that the assumption of zero water leaving radiance (L_w) in NIR channel of SeaWiFS was better justified. Moreover, the concept of BPA at NIR does not hold true in turbid coastal waters. Wang et al. (2009) showed that shifting BP to SWIR reduces the bias error but increases noise errors significantly. In A2 correction scheme, these assumptions were replaced by the assumption of spatial homogeneity of the 765 and 865 ratios for aerosol reflectance and for water leaving reflectance. Ruddick et al. (2000) reported that A1 scheme failed in the area of high TSM and CDOM. His theoretical analysis showed an error in estimation of normalized water leaving radiance (L_{wn}) and was of the order ± 0.01 for turbid water with turbid atmosphere. In the present study there was no significant difference between spectral R_{rs} derived using A1 and A2. This was probably due to the fact that the study area was more dominated by Chla having lesser impact of TSM and CDOM. The variability in spectral R_{rs} depends upon the variability in OAS as well as accurate computation of atmospheric radiances. The present study has addressed both the issues. The earlier study carried out by Menon et al. (2005) showed that higher concentration of Chla and CDOM significantly decrease L_w in shorter wavelength. In their study, Gordon and Wang (1994) estimated the effect of error induces in atmospheric correction using single scattering and multi scattering approximation. In the case of Chla derived using Gordon (1998) algorithm, they found the error of more than ± 20 % in all cases. Siegel et al. (2000) quantified the error that was due to the BPA for any arbitrary band ratio corresponding to SeaWiFS bands. Their result showed that for Chla less than 1 mg-m^{-3}, differences that are due to the application of NIR correction are less than 2 %. However for Chla greater than 2 mg-m^{-3}, band ratio error increases dramatically.

The validation of MODISA default bio-optical algorithm (OC3M) showed significant validation statistics. Although the statistical indicators showed moderate values, the accuracy of the algorithm was still in the acceptable limits. The OC3M algorithm was initially developed for case 1 waters eliminating the effect of OAS other than Chla. Its predicted accuracy was 70% in the open ocean (O'Reilly et al., 1998). In the present study 13 points were used for the validation. Further these match-up points cover the entire range of OAS encountered within the study area. These points were associated with a range of Chla concentration from 0.15 to 13.89 mg-m^{-3}, a_{CDOM}440 between 0.015 to 0.14 m^{-1} and TSM between 1.26 to 28.32 mg-l^{-1}. The statistical analysis indicates that the default atmospheric correction scheme (A1) was performing better. This was probably due to the fact that the concentration of TSM and CDOM was lower to overcome the impact of Chla. In the earlier studies carried out by Zhang et al. (2011) also showed that default algorithm for MODIS performs good in high Chla and TSM waters of Perl River Estuary where both the OAS were closely associated.

6. Conclusion

The present study was focused on the analysis of OAS in the coastal waters off Kochi, Southwest coast of India and also to evaluate the effect of OAS and atmospheric correction schemes on retrieval of spectral R_{rs} and Chla from MODISA data. The significant conclusions drawn from the study are as follows:

- The variability of OAS in the study area was attributed to the coastal upwelling and the fresh water discharge especially during southwest monsoon. Chla was the major light absorbing component in the study area. The distribution of OAS was highly variable, with maxima during southwest monsoon. The average value of $a_{CDOM}440$ was found to be on the lower side of the global mean. A significant negative relationship between $a_{CDOM}440$ and salinity during southwest monsoon indicates that much of the CDOM during this season was from river discharge. The spectral R_{rs} was found to be strongly linked to the variability in Chla concentration. With increase in Chla concentration, the peak R_{rs} was shifted to the longer wavelength.

- The validation of Chla, derived from *insitu* R_{rs}, showed moderate performance. However the accuracy of the algorithm was still in the acceptable limits.
- The spectral R_{rs} derived using atmospheric correction scheme, A1, was found to be in better agreement with *insitu*. Further Chla retrieved using A1 and A2 did not show any significant difference. This could be probably due to the fact that the study area was dominated by Chla with lower concentration of CDOM and TSM. The statistical analysis indicates that the default atmospheric correction scheme (A1) is performing better. Further the variability in R_{rs} and Chla retrieved using different atmospheric correction schemes has been well addressed.

7. Acknowledgement

This study was funded by Indian National Centre for Ocean Information Services (INCOIS), Ministry of Earth Sciences under SATellite Coastal Oceanographic REsearch (SATCORE) programme. The authors are thankful to the Directors of INCOIS and CIFT for the support and encouragement. The authors wish to acknowledge NASA-GSFC for making available MODIS – Aqua data. The authors are also grateful to managements & staffs of Bharathdarsan for their unrestricted support during the cruises. The authors also acknowledge the anonymous reviewers for their critical constructive comments. This is INCOIS contribution number 146.

8. References

Bailey, W. S., Werdell, J. P. 2006. A multi-sensor approach for the on-orbit validation of ocean color satellite data products. Remote Sensing of Environment, 102, 12−23

Balachandran, K. K. 2004. Does subterranean flow initiate mud banks off the southwest coast of India? Estuarine coastal and shelf science, 59; 589-598

Bukata R P, Jerome, J. H., Kondratyev, K. Y., and Pozdnyakov, D. V. 1995. Optical Properties and Remote Sensing of Inland and Coastal Waters; CRC Press Inc, New York.

Fargion, G.S. and J.L. Mueller, 2000: Ocean Optics Protocols for Satellite Ocean Color Sensor Validation, Revision 2, NASA/TM –2001-209955, NASA Goddard Space Flight Center, Greenbelt, Maryland. 184pp.

Gordon, H. R., & Morel, A. Y. 1983. Remote assessment of ocean colour for interpretation of satellite visible imagery: A review. New York' Springer-Verlag, 114 pp

Gordon, H. R., and Wang, M. 1994. Retrieval of water-leaving radiance and aerosol optical thickness over the oceans with SeaWiFS: a preliminary algorithm. Applied Optics, 33 (3): 443 – 452.

Gordon, H.R. (1998) In-orbit calibration strategy for ocean color sensors (1998) Remote Sensing of Environment, 63 (3), pp. 265-278

Habeebrehman, H., Prabhakaran, M. P., Josia Jacob., Sabu P., Jayalakshmi, K. J., Achuthankutty, C.T., Revichandran, C. 2008. Variability in biological responses influenced by upwelling events in the eastern Arabian Sea. Journal of Marine Systems, 74, 545-560

Hareesh Kumar, P.V. and Mohan Kumar, N., 1996. On the flow and thermohaline structure off Cochin during pre-monsoon season Continental Shelf Research, 16(4), 457-468.

IOCCG. 2000. Remote Sensing of Ocean Colour in Coastal, and Other Optically-Complex, Waters. Sathyendranath, S. (ed.), Reports of the International Ocean-Colour Coordinating Group, No. 3, IOCCG, Dartmouth, Canada.

Joshi M., Rao, A. D. 2012. Response of Southwest monsoon winds on shelf circulation off Kerala coast, India. Continental shelf Research, 32, 62-70

Jyothibabu, R., Madhu, N. V., Jayalakshmi, K.V., Balachandran, K.K., Shiyas, C.A., Martin, G.D., Nair, K.K.C. 2006. Impact of fresh water influx on microzooplankton mediated food web in a tropical estuary (Cochin backwaters - India). Estuarine, Coastal and Shelf Science, 69: 505 - 518.

Kowalczuk, P., Kaczmark, S. 1996: Analysis of temporal and spatial variability of Yellow Substance absorption in the southern Baltic. Oceanologia

Lévy, M., Shankar, D., André, J.-M., Shenoi, S.S.C., Durand, F., de Boyer Montégut, C. 2007. Basin-wide seasonal evolution of the Indian Ocean's phytoplankton blooms. Journal of Geophysical Research (C): Oceans, 112 (12)

Menon, H.B., Lotliker, A., Nayak, S.R. 2005. Pre-monsoon bio-optical properties in estuarine, coastal and Lakshadweep waters. Estuarine, Coastal and Shelf Science, 63 (1-2), 211-223

Menon, H.B., Sangekar, N.P., Lotliker, A.A., Vethamony, P. 2011. Dynamics of chromophoric dissolved organic matter in Mandovi and Zuari estuaries - A study through in situ and satellite data. ISPRS Journal of Photogrammetry and Remote Sensing, 66 (4), 545-552

Morel A, Prieur L. 1977. Analysis of variations in ocean color. Limnology and Oceanography, 22(4), 709–722

Nair, S. S., Devassy, V.P., Madhupratap, M. 1992. Blooms of phytoplankton along the west coast of India associated with nutrient enrichment and the response of zooplankton. Science of the Total Environment, 26: 819–828.

O'Reilly, J. E., S. Maritorena, D. Siegel, M. C. O'brien, D. Toole, B. G. Mitchell, M. Kahru, F. P. Chavez, P. Strutton, G. Cota, S. B. Hooker, C. R. McClain, K. L. Carder, F. Muller-Karger, L. Harding, A. Magnuson, D. Phinney, G. F. Moore, J. Aiken, K. R. Arrigo, R. Letelier, and M. Culver. 2000. Ocean color chlorophyll a algorithms for SeaWiFS, OC2, and OC4: Version 4. In: Hooker S. B. and E. R. Firestone (Eds.), SeaWiFS Postlaunch Technical Report Series, SeaWiFS Post-launch Calibration and Validation Analyses, Volume 11, Part 3, 9-23, Greenbelt, Maryland: NASA Goddard Space Flight Center, 1-51.

O'Reilly, J.E., Maritorena, S., Mitchell, B.G., Siegel, D.A., Carder, K.L., Garver, S.A., Kahru, M., and McClain, C.R. 1998. Ocean colour chlorophyll algorithms for SeaWiFS: Journal of Geophysical Research, 103, 24937-24953.

Ruddick, K. G., F. Ovidio, M. Rijkeboer. 2000. Atmospheric correction of SeaWiFS imagery for turbid coastal and inland waters. Applied Optics, 39, 897–912.

Sarupria J S., Bhargava R M S. 1993. Seasonal Primary Production in Different Sectors of the EEZ of India Mahasagar 26, 139-147

Shankar, D., Vinayachandran, P.N., and Unnikrishnan, A.S. 2002. The monsoon currents in the north Indian Ocean. Progress in Oceanography, 52, 63-120

Siegel, D.A., Maritorena, S., Nelson, N.B., Hansell, D.A., Lorenzi-Kayser, M., 2002. Global distribution and dynamics of colored dissolved and detrital organic materials. J. Geophys. Res. Oceans 107 (C12). doi:10.1029/2001JC000965.

Siegel, D. A.,Wang, M., Maritorena, S., Robinson,W. 2000. Atmospheric correction of satellite ocean color imagery: The black pixel assumption. Applied Optics, 39, 3582−3591

Siegel, D., and A. Michaels. 1996. Quantification of non-algal light attenuation in the Sargasso Sea: Implications for biogeochemistry and remote sensing, Deep Sea Res., Part II, 43, 321-345,

Srinivas K., Dineshkumar, P. K. 2006. Atmospheric forcing on the seasonal variability of sea level at Cochin, South west of India. Continental Shelf Research, 26, 1113-1133

Srinivas, K., Revichandran, C., Maheswaran, P.A., Ashraf, M. T.T., Murukesh, N. 2003. Propagation of tides in the Cochin estuarine system South west coast of India. Indian Journal of Marine Sciences, 32(1): 14-24**.**

Stramski, D., Tegowski, J. 2001. Effects of intermittent entrainment of air bubbles by breaking wind waves on ocean reflectance and underwater light field. Journal of Geophysical Research, 106, 31345–31360

Strickland, J. D., Parson, T. R. 1972. A Practical handbook of Seawater Analysis. Bulletin of Fishery Research Board, Canada: 167 – 310.

Terrill, E. J., Melville, W. K., Stramski, D. 2001. Bubble entrainment by breaking waves and their influence on optical scattering in the upper ocean. Journal of Geophysical Research, 106, 16815–16823.

Thomas, J.V., Premlal, P., Sreedevi, C., Kurup, M. B. 2004. Immediate effect of bottom trawling on the physicochemical parameters in the inshore waters (Cochin-Munambum) of Kerala. Indian Journal of Fisheries, 51(3): 277-286.

Twardowski, M.S., Boss, E., Sullivan, J.M., & Donaghay, P.L. 2004. Modeling the spectral shape of absorption by chromophoric dissolved organic matter. Marine Chemistry, 89, 69-88

UNESCO. 1994. Protocols for joint global ocean carbon flux study (JGOFS) core measurements.

Wang, M., Son, S., Shi, W. 2009. Evaluation of MODIS SWIR and NIR–SWIR atmospheric correction algorithms using SeaBASS data. Remote Sensing of Environment, 113, 635−644

Wang, M., W. Shi. 2005. Estimation of ocean contribution at the MODIS near-infrared wavelengths along the east coast of the US.: Two case studies, Geophysical Research Letters, 32, L13606, doi: 10.1029/ 2005GL022917

Welschmeyer, N.A. 1994. Fluorometric analysis of chlorophyll a in the presence of chlorophyll b and pheopigments. Limnology and Oceanography, 39, 1985-1992

Zhang, Y., Lin, H., Chen, C., Chen, L., Zhang, B., Gitelson, A. A. 2011. Estimation of chlorophyll-a concentration in estuarine waters: case study of the Pearl River estuary, South China Sea. Environment Research Letters, 6, doi:10.1088/1748-9326/6/2/024016

Zibordi, G., Melin, F., Berthon, J.F., 2006. Comparison of SeaWiFS, MODIS and MERIS radiometric products at a coastal site Geophysical Research Letters 33 (6)

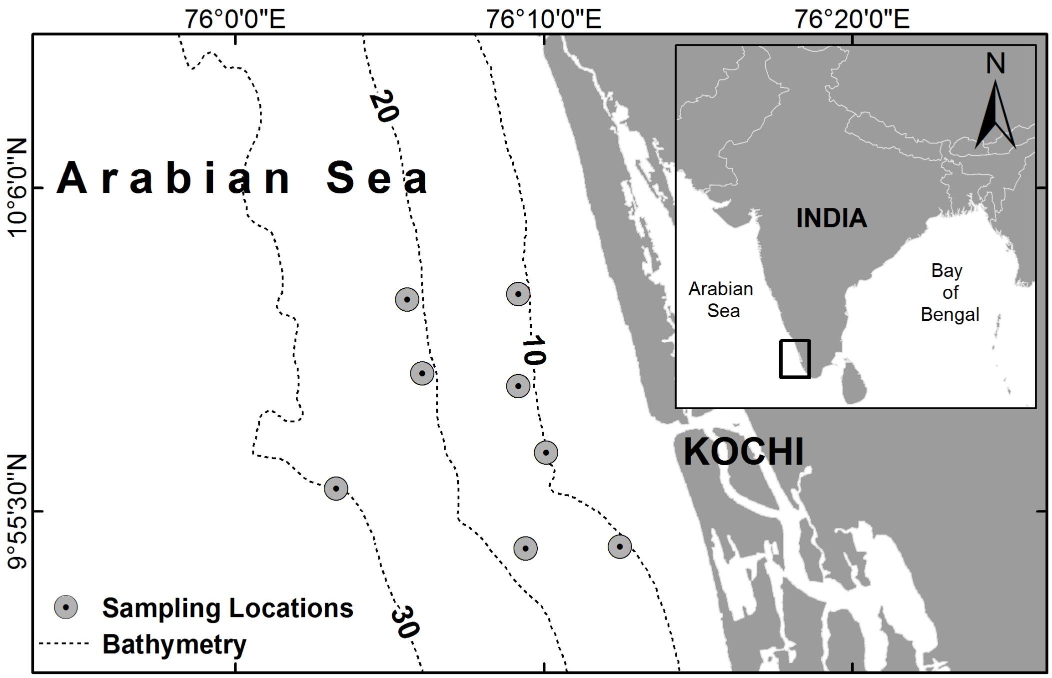

Figure 1: Map of Study Area showing the sampling locations

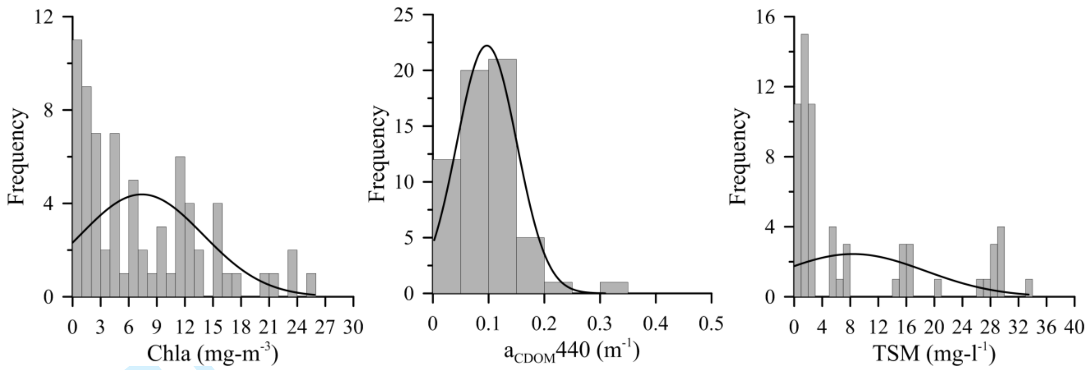

Figure 2: Frequency distribution of Chlorophyll_a (Chla), absorption due to Chromophoric Dissolved Organic Matter at 440 nm ($a_{CDOM}440$) and Total Suspended Sediment (TSM) in the study area for the entire sampling period. The curve indicates the normal distribution.

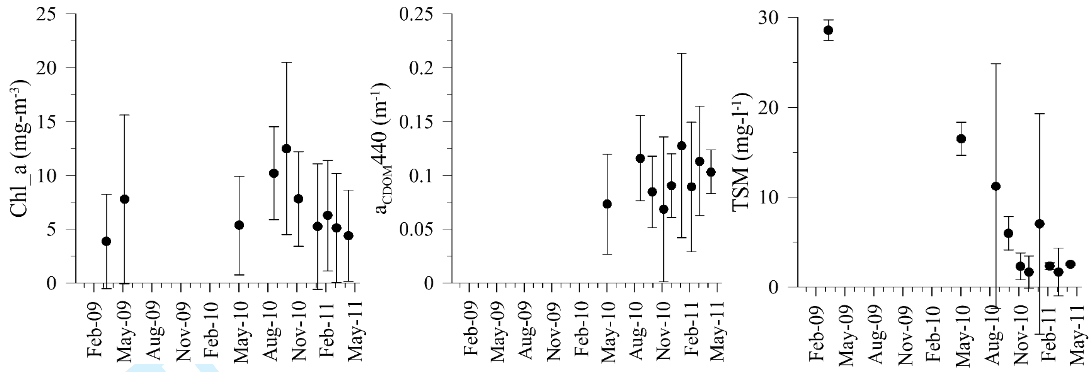

Figure 3: Monthly mean distribution of Chlorophyll_a (Chla), absorption due to Chromophoric Dissolved Organic Matter at 440 nm ($a_{CDOM}440$) and Total Suspended Sediment (TSM) in the study area. The vertical bars indicate standard deviation.

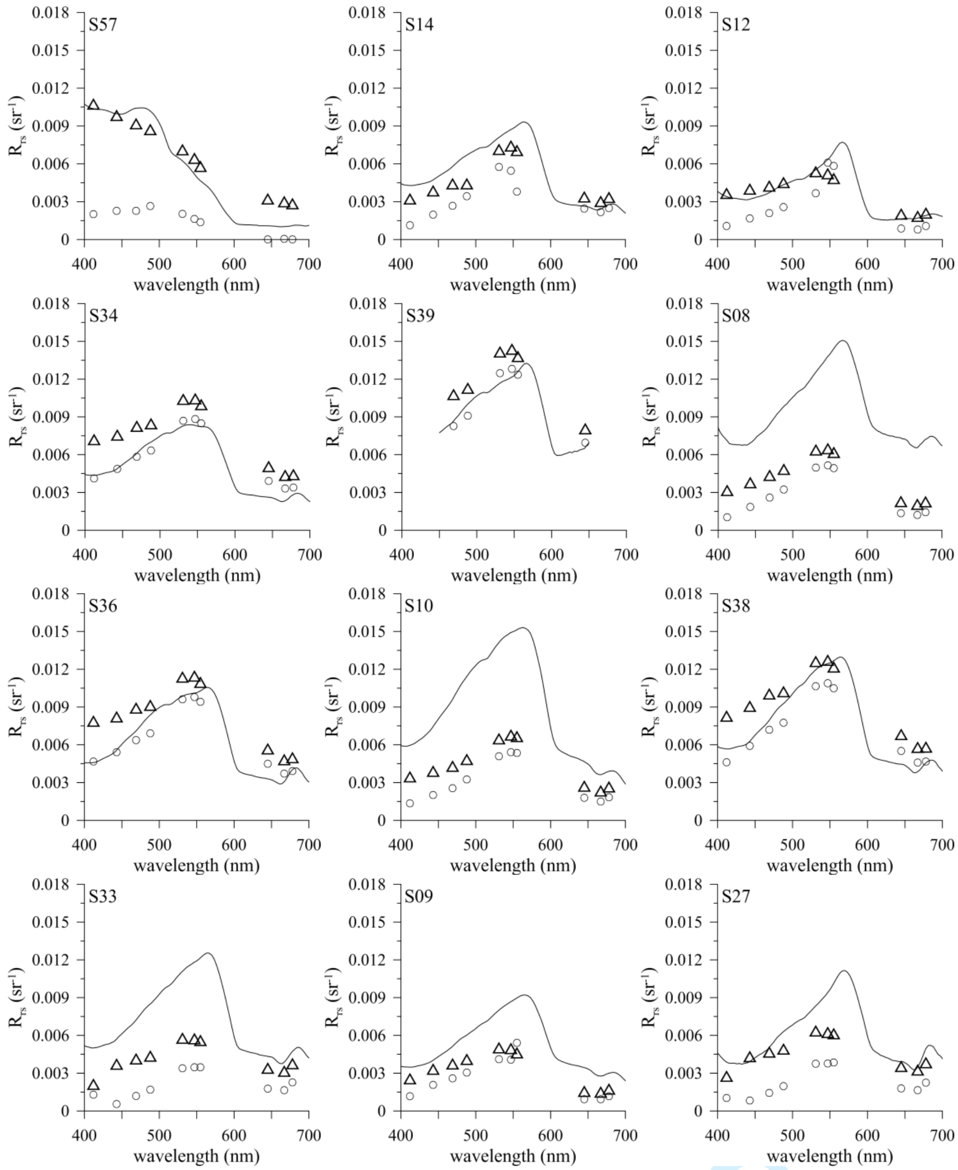

Figure 4: Spectral variability in remote sensing reflectance (R_{rs}) measured *insitu*, using hyperspectral radiometer (solid line) and that derived from satellite data using two atmospheric correction schemes, at stations selected for validation. The triangles represents R_{rs} derived using 2-band model selection and iterative NIR correction. The circles represents R_{rs} derived using 2-band model selection and MUMM NIR correction.

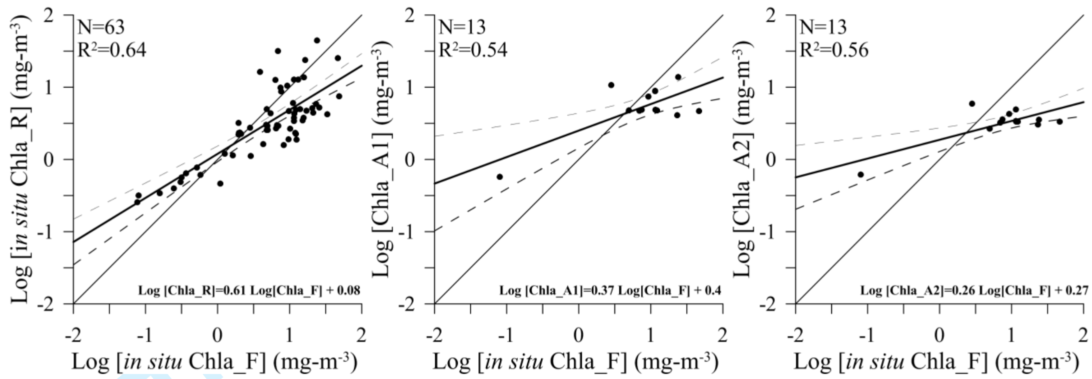

Figure 5: Correlation between *insitu* measured Chla and a) Chla estimated using Rrs from radiometer data, b) Chla generated from satellite data using 2-band model selection and iterative NIR correction and c) 2-band model selection and MUMM NIR correction. In all cases OC3M algorithm was used to estimate Chla. The thin solid line represents perfect linear fit. The thick solid line represents the linear data trend. The dotted line represents the 95% confidence limit.

Table 1: Statistical indicators for evaluation of Chla. The first row is the analysis between *insitu* Chla and that derived using OC3M algorithm from *insitu* R_{rs}. The second and third row represents analysis between *insitu* measured Chla and satellite derived Chla using OC3M algorithm and two different atmospheric correction schemes. The atmospheric correction schemes used are (A1) 2-band model selection and iterative NIR correction and (A2) 2-band model selection and MUMM NIR correction. The statistical evaluation was carried out at 95% confidence level.

	N	R^2	SLOPE	INTERCEPT	r	Log RMSE	APD	RPD
Chl Radiometer (Chl_R)	63	0.64	0.61	0.08	1.806	0.434	43.60	42.33
Chl Atm1 (Chl_A1)	13	0.54	0.37	0.40	1.611	0.49	25.46	17.57
Chl Atm2 (Chl_A2)	13	0.56	0.26	0.27	2.176	0.62	40.01	41.43